

Organic biomorphs may be better preserved than microorganisms in early Earth sediments

Christine Nims^{1*}, Julia Lafond¹, Julien Alleon², Alexis S. Templeton³ and Julie Cosmidis^{1†}

¹Department of Geosciences, Pennsylvania State University, University Park, Pennsylvania 16802, USA

²Faculté des Géosciences et de l'Environnement, Institut des Sciences de la Terre, Université de Lausanne, CH-1015 Lausanne, Switzerland

³Department of Geological Sciences, UCB 399, University of Colorado, Boulder, Colorado 80309, USA

ABSTRACT

The Precambrian rock record contains numerous examples of microscopic organic filaments and spheres, commonly interpreted as fossil microorganisms. Microfossils are among the oldest traces of life on Earth, making their correct identification crucial to our understanding of early evolution. Yet, spherical and filamentous microscopic objects composed of organic carbon and sulfur can form in the abiogenic reaction of sulfide with organic compounds. Termed organic biomorphs, these objects form under geochemical conditions relevant to the sulfidic environments of early Earth. Furthermore, they adopt a diversity of morphologies that closely mimic a number of microfossil examples from the Precambrian record. Here, we tested the potential for organic biomorphs to be preserved in cherts; i.e., siliceous rocks hosting abundant microbial fossils. We performed experimental silicification of the biomorphs along with the sulfur bacterium *Thiothrix*. We show that the original morphologies of the biomorphs are well preserved through encrustation by nano-colloidal silica, while the shapes of *Thiothrix* cells degrade. Sulfur diffuses from the interior of both biomorphs and *Thiothrix* during silicification, leaving behind empty organic envelopes. Although the organic composition of the biomorphs differs from that of *Thiothrix* cells, both types of objects present similar nitrogen/carbon ratios after silicification. During silicification, sulfur accumulates along the organic envelopes of the biomorphs, which may promote sulfurization and preservation through diagenesis. Organic biomorphs possessing morphological and chemical characteristics of microfossils may thus be an important component in Precambrian cherts, challenging our understanding of the early life record.

INTRODUCTION

Reconstructing the early history of life on Earth relies on our ability to identify the remnants of microorganisms in the rock record. Traces of ancient microbial life can be chemical (e.g., biologically derived organic compounds or isotopic signals) or morphological (e.g., microfossils), but their correct identification is rife with challenges (Schopf et al., 2010; Javaux, 2019). One of the main issues is the potential for abiotic processes to generate microstructures mimicking prokaryotic cell morphologies, and thus create “false positive” evidence of early

life in the geological record. Different types of microstructures emulating microbial cells have been described from laboratory-based (Fox and Yuyama, 1963; Barge et al., 2016; McMahon, 2019; García-Ruiz et al., 2020) and field-based (Brasier et al., 2002; Marshall et al., 2011; Wacey et al., 2018) studies. Recently, organic microstructures bearing both morphological and chemical resemblance to microbial filamentous and spherical cells were synthesized experimentally (Cosmidis and Templeton, 2016). These objects, called here organic biomorphs, self-assemble when sulfide is oxidized in the presence of organics. They form spontaneously in a wide range of geochemical conditions relevant to modern and ancient sulfidic environments. Furthermore, the organic biomorphs form from diverse organic compounds, including simple prebiotic organics (e.g., glycine) (Cosmidis

et al., 2019), and so possibly assembled in Earth's early environments prior to the origin of life.

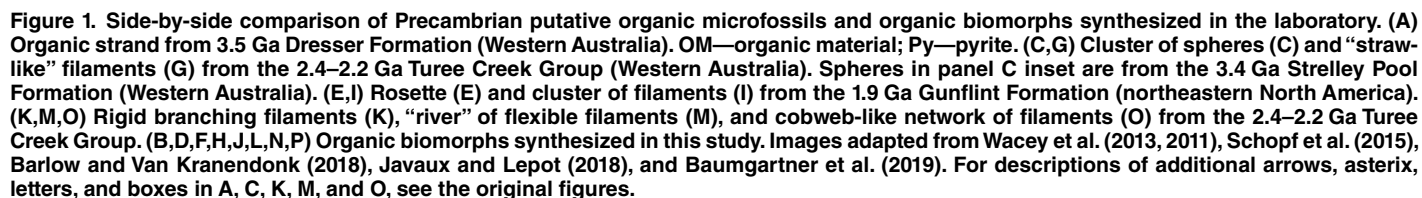
Figure 1 compares the morphologies of laboratory-synthesized organic biomorphs with putative organic microfossils from the Archean and Proterozoic record, namely the 3.5 Ga Dresser Formation (Baumgartner et al., 2019) (Fig. 1A), 3.4 Ga Strelley Pool Formation (Wacey et al., 2011) (subset in Fig. 1C), and 2.4–2.2 Ga Turee Creek Group (Schopf et al., 2015; Barlow and Van Kranendonk, 2018) (Figs. 1C, 1G, 1K, 1M, and 1O) of Western Australia, and the 1.9 Ga Gunflint Formation (Wacey et al., 2013) (Figs. 1E and 1I) in northeastern North America. Organic biomorphs shown for comparison include (1) spheroids, either isolated or clustered (Fig. 1D); (2) tubes or filaments, either rigid (Figs. 1J and 1L) or flexible (Figs. 1B and 1N), in some cases branching (Fig. 1L) or forming angles (Fig. 1H), isolated (Fig. 1H), clustered (Fig. 1J), or forming “rivers” (Fig. 1N) or tangled networks (Fig. 1P); and (3) rosettes of filaments (Fig. 1F).

These morphological similarities are insufficient for disproving the biogenicity of the putative microfossils exemplified here, which in some cases has been well established (e.g., the Gunflint microfossils; Lepot et al., 2017). Yet, this comparison clearly cautions against using morphological criteria for identifying microfossils, especially in rocks marked by sulfide-rich conditions.

Euxinic conditions were common in Proterozoic oceans (Lyons et al., 2009), and reduced sulfur species could have been locally concentrated in Archean sedimentary environments despite low global oceanic sulfate (e.g., Marin-Carbonne et al., 2018). Precambrian microfossils such as those shown in Figure 1 are commonly closely associated with pyrite (e.g., Wacey et al.,

*Current address: Earth and Environmental Sciences, University of Michigan, Ann Arbor, Michigan 48109-1005, USA.

†Current address: Department of Earth Sciences, University of Oxford, South Parks Road, Oxford OX1 3AN, UK; E-mail: julie.cosmidis@earth.ox.ac.uk.



Organic biomorphs were obtained by reacting sulfide in solution with dissolved yeast extract (a complex organic mixture) under sterile conditions. Following earlier experimental silicification protocols (Toporski et al., 2002; Benning et al., 2004), the biomorphs were dispensed into a sterile supersaturated

sodium-metasilicate solution and stored at room temperature for up to five months. The same procedure was applied to freshly collected mats of *Thiothrix* sp., a filamentous sulfur-oxidizing bacterium (Larkin and Strohl, 1983). Samples were collected at different times during silicification and characterized using scanning electron microscopy (SEM) and transmission electron microscopy (TEM) coupled with energy-dispersive X-ray spectroscopy (EDS), Raman spectroscopy, attenuated total reflectance–Fourier transform infrared spectroscopy (ATR-FTIR), X-ray absorption near-edge structure (XANES) at the sulfur K-edge, and scanning transmission X-ray microscopy (STXM) at the carbon K-edge, nitrogen K-edge, and sulfur L-edge. See the Supplemental Material¹ for full details.

RESULTS AND DISCUSSION

The biomorphs used for silicification consisted of spheres (0.5–3 μm in diameter) interspersed with filaments (0.1–1 μm thick). As experimental silicification proceeded, the spherical biomorphs mostly retained their original morphology, while silicified *Thiothrix* cells rapidly evolved from cylindrical shapes into deformed, flattened ribbons (Fig. 2). Deflated cells are not artifacts of sample preparation or imaging mode, given that non-silicified *Thiothrix* cells retained their cylindrical shapes in SEM images. On the contrary, despite some fragmentation during silicification, many filamentous biomorphs remained intact four weeks after the beginning of the experiment (Fig. 2D). The biomorphs were morphologically preserved by rapid (within 24 h) precipitation of nano-colloidal silica on their surfaces (Fig. 2B), eventually forming a thin crust around the spheres and the filaments (Fig. 3). In contrast, a thick silica gel formed around *Thiothrix* cells (Fig. 2G). This difference in the extent of silica polymerization may be attributed to the presence of extracellular polymeric substances around *Thiothrix* (Benning et al., 2004; Lalonde et al., 2005), or to metabolic activity of the cells, which initially decreased the pH of the silicification medium, increasing silica saturation (Fig. S1 in the Supplemental Material). In contrast, the pH of biomorph silicification medium remained constant at pH 7 (± 0.5 pH units) throughout the experiment.

Elemental sulfur, initially present as intracellular amorphous globules inside *Thiothrix*, progressively diffused from the cells during silicification (Fig. 3). Many sulfur-depleted *Thiothrix* filaments were observed one week into the experiment, while sulfur reprecipitated as the metastable allotrope $\beta\text{-S}_8$ in the extracel-

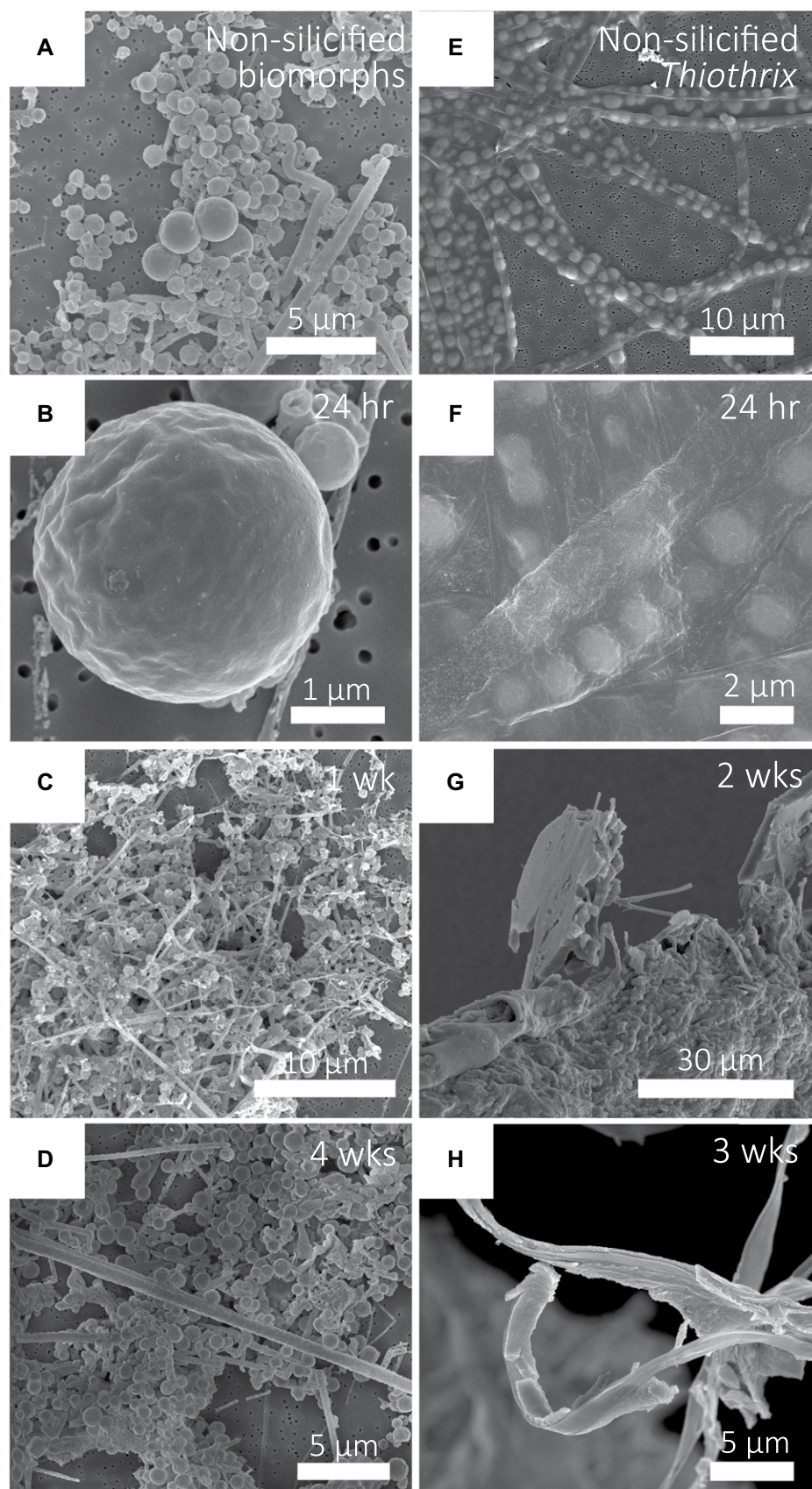


Figure 2. Scanning electron microscopy images of organic biomorphs (A–D) and sulfur bacterium *Thiothrix* cells (E–H) prior to and at different times throughout silicification. Note the silica nano-colloids at the surfaces of spherical biomorph in B and of *Thiothrix* filaments in F.

¹Supplemental Material. Detailed materials and methods, supplemental text, and Figures S1–S4. Please visit <https://doi.org/10.1130/GEOL.S.13530692> to access the supplemental material, and contact editing@geosociety.org with any questions.

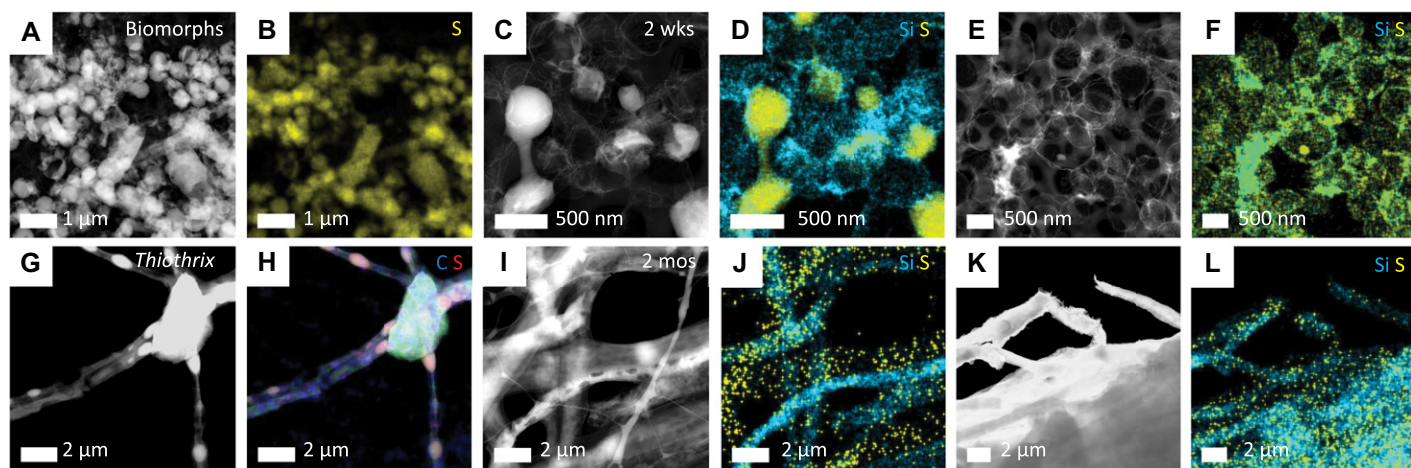


Figure 3. High-resolution imaging and chemical mapping of organic biomorphs and sulfur bacterium *Thiothrix* cells throughout silicification. (A–F) High-angle annular dark field–scanning transmission electron microscopy (HAADF-STEM) images and corresponding energy-dispersive X-ray spectroscopy (EDS) maps of biomorphs prior to silicification (A,B) and two weeks into silicification (C–F). (G–L) HAADF-STEM images and corresponding EDS maps of *Thiothrix* cells prior to (G,H) and two months into (I–L) silicification. EDS maps show distribution of sulfur in yellow and silica in cyan, except in H, where carbon is in blue and sulfur in red.

lular medium (Fig. S2). Likewise, sulfur diffused from the biomorphs during silicification, leaving behind empty organic vesicles (Fig. 3), but it also accumulated along the envelope of the silicified biomorphs (Fig. 3F). Originally enclosed as γ -S₈, sulfur re-precipitated post-silicification as α -, β -, and γ -S₈ (Fig. S2). Sulfur K-edge XANES spectroscopy also identified oxidized sulfur (sulfate, thiosulfate, and/or sulfones and ester sulfates) associated with silicified biomorphs (Fig. S3, and Supplemental Material text).

Sulfur diffusion from *Thiothrix* cells and biomorphs during silicification indicates solubilization, most likely as polysulfides (Kleinjan et al., 2005). Polysulfides are highly reactive toward organics, causing rapid organic-matter sulfuration (Raven et al., 2016). The sulfur-rich organic envelopes of the silicified biomorphs (Fig. 3F) may indicate sulfuration, and ATR-FTIR analysis showed the formation of sulfur-bearing groups such as organic sulfates and sulfonic groups during silicification. However, intramolecular sulfur incorporation in silicified biomorphs could not be confirmed due to possible interference with siloxane groups (see Fig. S4, and Supplemental Material text). Early diagenetic sulfuration favors the preservation of organic microstructures in ancient rocks (Lepot et al., 2009), so determining whether organic biomorphs can be sulfurized will aid in the evaluation of their preservation potential.

We note that the sulfur loss from the organic biomorphs during silicification would likely give rise to chert-hosted organic microstructures that do not contain sulfur-bearing minerals. Instead, in iron- and sulfide-rich environments, the diffusion of polysulfides from the biomorphs would result in pyrite precipitation in their close vicinity (Rickard and Luther, 2007), as is commonly observed in chert-hosted ancient organic micro-

structures (e.g., Wacey et al., 2011, 2013; Schopf et al., 2015; Baumgartner et al., 2019).

As determined using ATR-FTIR (Fig. S4) and STXM (Fig. 4), the organic composition of the biomorphs prior to silicification was dominated by carboxylic groups and unsaturated carbon, along with aliphatics, alcohols, and C = O groups. As silicification proceeded, the aliphatic, aromatic, and unsaturated carbon content of the biomorphs increased, while signals from other organic components decreased. In contrast, the spectroscopic signature of both native and silicifying *Thiothrix* cells was dominated by amide groups from proteins. Previous studies have shown that amides can be incorporated into organic biomorphs when peptides are present in their synthesis medium (Cosmidis and Templeton, 2016). Here, amides were not detected in the biomorphs, although they formed in the presence of yeast extract, which contains peptides. Nitrogen in the biomorph envelope was instead present in an unidentified inorganic or organic form (see the Supplemental Material). Thus, carbon and nitrogen speciations of the *Thiothrix* cells versus the biomorphs are notably different.

The initial nitrogen/carbon (N/C) ratio of the biomorphs, determined using STXM (Alleon et al., 2015), was 0.27 ± 0.02 before silicification and increased to 0.40 ± 0.02 after silicification (Fig. 4I). The initial N/C ratio of *Thiothrix* cells was 0.16 ± 0.02 (within the range of previously measured bacteria; Alleon et al., 2017). This ratio increased after one week of silicification to 0.42 ± 0.02 , a value similar to that of silicified biomorphs, but higher than N/C values reported for Precambrian microfossils (0.09–0.25) (Alleon et al., 2016b, 2018). It remains to be determined how the organic composition and N/C ratio of the silicified biomorphs may be affected by diagenesis at high tempera-

ture and pressure (e.g., Alleon et al., 2016a). Differences in the molecular compositions of the biomorphs compared with microbial cells may lead to different chemical behaviors during diagenesis, allowing for fossil biomorphs and bacteria to be distinguished in rocks based on their thermally matured residues (Alleon et al., 2017).

CONCLUSIONS

Organic biomorphs that form via the abio-genic reaction of sulfide with organics are likely to be preserved as pseudofossils in cherts through rapid silica encrustation and, possibly, organic-matter sulfuration. In addition to their striking morphological resemblance to putative Precambrian microfossils, these pseudofossils would share chemical characteristics with actual fossil bacteria, such as complex organic compositions and presence of nitrogen atoms. Importantly, organic biomorphs demonstrate better morphological preservation compared with microbial cells during silicification.

While these findings do not refute previous interpretations of Precambrian putative microfossils, our results call for a circumspect approach when evaluating the biogenicity of chert-hosted organic microstructures. In particular, a bacterial morphology, even when associated with an organic composition, can no longer inform biogenicity, especially in geochemical contexts indicative of sulfidic environments. We argue for a concerted effort to better identify potential abiosignatures (i.e., signatures of abiotic processes) (Chan et al., 2019) in the geological record, particularly those that mimic genuine biosignatures. This work is fundamental to avoiding potential pitfalls of biological “false positives” and increasing confidence in our ability to detect life in ancient rocks and astrobiological explorations.

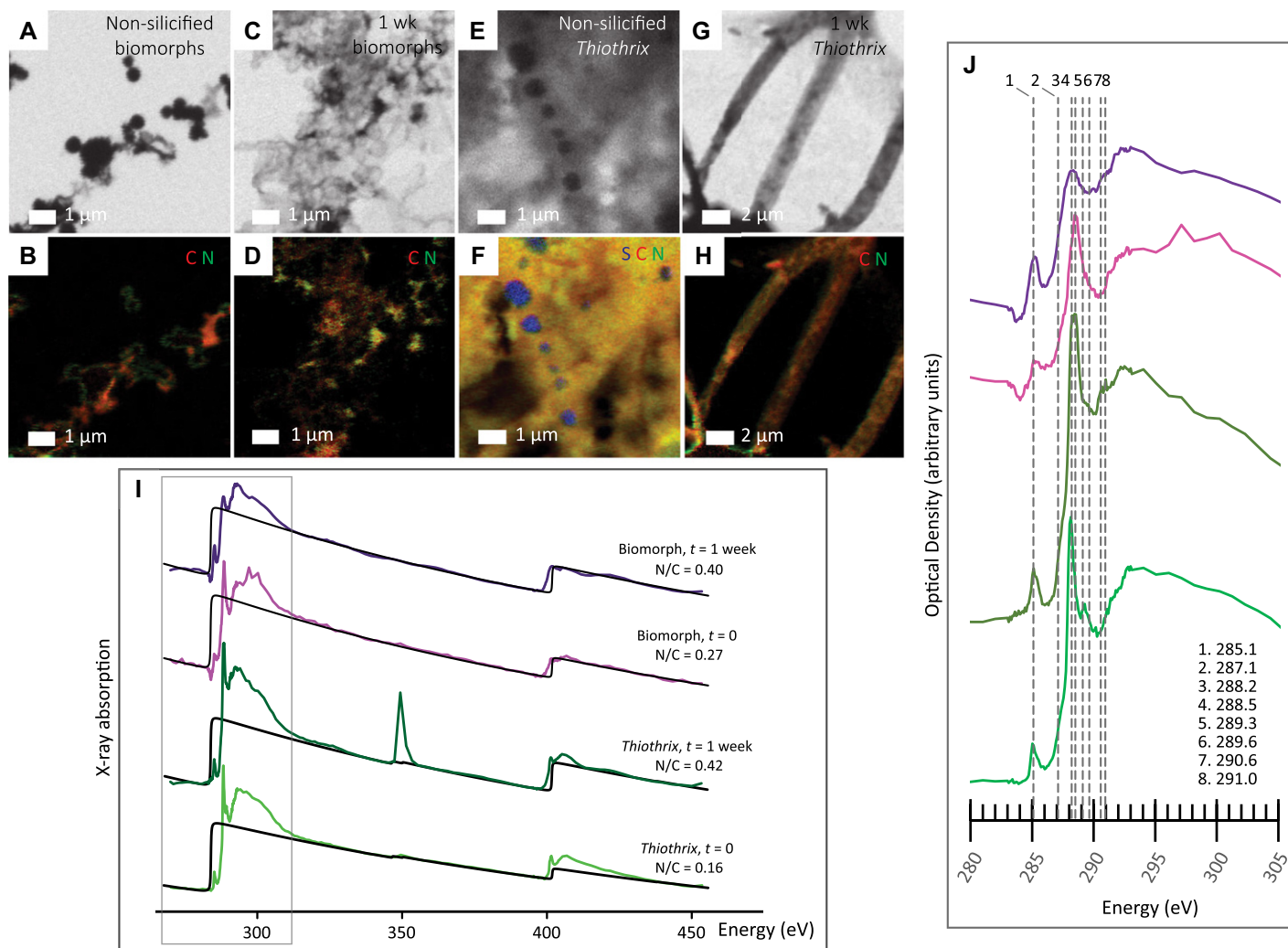


Figure 4. Scanning transmission X-ray microscopy (STXM) analyses of organic biomorphs and sulfur bacterium *Thiothrix* cells prior to and one week into silicification. (A–H) STXM images and corresponding STXM chemical maps of biomorphs (A–D) and *Thiothrix* (E–H). Pre-silicification images A and E show dense sulfur spheres inside spherical biomorphs and *Thiothrix* cells. STXM maps (B,D,F,H) show distribution of carbon (red), nitrogen (green), and sulfur (blue; in F only). (I) X-ray absorption near-edge structure (XANES) spectra covering carbon (C) and nitrogen (N) K-edges, and calculated N/C ratios. Black rectangle shows the carbon K-edge spectral range (closeup in J). Black curves show the fitting functions for N/C ratio calculations as described by Alleon et al. (2015). Spectrum of silicified *Thiothrix* includes a feature at ~350 eV, corresponding to calcium. (J) Closeup of carbon K-edge XANES spectra. Energies of the main absorbance features are indicated.

ACKNOWLEDGMENTS

We thank Jennifer Williams (Pennsylvania State University [PSU]) for her help with the collection of *Thiothrix* samples; Brandi Cron and Jennifer Macalady (PSU) for assistance with their taxonomic identification; Maxwell Wetherington (PSU) for his help with Raman analyses; and Tawanda (TJ) Zimudzi (PSU) for his help with FTIR measurements. Sulfur K-edge XANES analyses were performed on beamline 4–3 of the Stanford Synchrotron Radiation Light-source (SSRL; Stanford, California, USA) with the assistance of Matthew Latimer and Erik Nelson. Use of the SSRL, SLAC National Accelerator Laboratory, is supported by the U.S. Department of Energy, Office of Science, Office of Basic Energy Sciences under contract DE-AC02-76SF00515. The contents of this publication are solely the responsibility of the authors and do not necessarily represent the official views of the U.S. National Institute of General Medical Sciences or the National Institutes of Health. We thank Jian Wang for his support on beamline SM of the Canadian Light Source (CLS; Saskatoon, Saskatchewan, Canada). CLS is supported by the Canada

Foundation for Innovation, Natural Sciences and Engineering Research Council of Canada, the University of Saskatchewan, the Government of Saskatchewan, Western Economic Diversification Canada, the National Research Council Canada, and the Canadian Institutes of Health Research. This work was supported through startup funding provided by the PSU Department of Geosciences to Cosmidis, following on preliminary work supported by the NASA Astrobiology Institute Co-operative Agreement NN15BB02A. We thank Craig Marshall and an anonymous reviewer for their insightful comments.

REFERENCES CITED

- Alleon, J., Bernard, S., Remusat, L., and Robert, F., 2015, Estimation of nitrogen-to-carbon ratios of organics and carbon materials at the submicrometer scale: *Carbon*, v. 84, p. 290–298, <https://doi.org/10.1016/j.carbon.2014.11.044>.
- Alleon, J., Bernard, S., Le Guillou, C., Daval, D., Skouri-Panet, F., Pont, S., Delbes, L., and Robert, F., 2016a, Early entombment within silica minimizes the molecular degradation of microorgan-

isms during advanced diagenesis: *Chemical Geology*, v. 437, p. 98–108, <https://doi.org/10.1016/j.chemgeo.2016.05.034>.

- Alleon, J., Bernard, S., Le Guillou, C., Marin-Carbonne, J., Pont, S., Beyssac, O., McKeegan, K.D., and Robert, F., 2016b, Molecular preservation of 1.88 Ga Gunflint organic microfossils as a function of temperature and mineralogy: *Nature Communications*, v. 7, 11977, <https://doi.org/10.1038/ncomms11977>.
- Alleon, J., Bernard, S., Le Guillou, C., Daval, D., Skouri-Panet, F., Kuga, M., and Robert, F., 2017, Organic molecular heterogeneities can withstand diagenesis: *Scientific Reports*, v. 7, 1508, <https://doi.org/10.1038/s41598-017-01612-8>.
- Alleon, J., Bernard, S., Le Guillou, C., Beyssac, O., Sugitani, K., and Robert, F., 2018, Chemical nature of the 3.4 Ga Strelley Pool microfossils: *Geochimica et Cosmochimica Acta*, v. 228, p. 37–42, <https://doi.org/10.1016/j.gca.2018.07.017>.
- Barge, L.M., Cardoso, S.S.S., Cartwright, J.H.E., Doloboff, I.J., Flores, E., Macías-Sánchez, E., Sainz-Díaz, C.I., and Sobrón, P., 2016,

- Self-assembling iron oxyhydroxide/oxide tubular structures: Laboratory-grown and field examples from Rio Tinto: *Proceedings of the Royal Society [London]: A, Mathematical, Physical and Engineering Sciences*, v. 472, 20160466, <https://doi.org/10.1098/rspa.2016.0466>.
- Barlow, E.V., and Van Kranendonk, M.J., 2018, Snapshot of an early Paleoproterozoic ecosystem: Two diverse microfossil communities from the Turee Creek Group, Western Australia: *Geobiology*, v. 16, p. 449–475, <https://doi.org/10.1111/gbi.12304>.
- Baumgartner, R.J., Van Kranendonk, M.J., Wacey, D., Fiorentini, M.L., Saunders, M., Caruso, S., Pages, A., Homann, M., and Guagliardo, P., 2019, Nano-porous pyrite and organic matter in 3.5-billion-year-old stromatolites record primordial life: *Geology*, v. 47, p. 1039–1043, <https://doi.org/10.1130/G46365.1>.
- Benning, L.G., Phoenix, V.R., Yee, N., and Konhauser, K.O., 2004, The dynamics of cyanobacterial silicification: An infrared micro-spectroscopic investigation: *Geochimica et Cosmochimica Acta*, v. 68, p. 743–757, [https://doi.org/10.1016/S0016-7037\(03\)00488-5](https://doi.org/10.1016/S0016-7037(03)00488-5).
- Brasier, M.D., Green, O.R., Jephcoat, A.P., Kleppe, A.K., Van Kranendonk, M.J., Lindsay, J.F., Steele, A., and Grassineau, N.V., 2002, Questioning the evidence for Earth's oldest fossils: *Nature*, v. 416, p. 76–81, <https://doi.org/10.1038/416076a>.
- Chan, M.A., et al., 2019, Deciphering biosignatures in planetary contexts: *Astrobiology*, v. 19, p. 1075–1102, <https://doi.org/10.1089/ast.2018.1903>.
- Cosmidis, J., and Templeton, A.S., 2016, Self-assembly of biomorphic carbon/sulfur microstructures in sulfidic environments: *Nature Communications*, v. 7, 12812, <https://doi.org/10.1038/ncomms12812>.
- Cosmidis, J., Nims, C.W., Diercks, D., and Templeton, A.S., 2019, Formation and stabilization of elemental sulfur through organomineralization: *Geochimica et Cosmochimica Acta*, v. 247, p. 59–82, <https://doi.org/10.1016/j.gca.2018.12.025>.
- Fox, S.W., and Yuyama, S., 1963, Abiotic production of primitive protein and formed microparticles: *Annals of the New York Academy of Sciences*, v. 108, p. 487–494, <https://doi.org/10.1111/j.1749-6632.1963.tb13404.x>.
- García-Ruiz, J.M., van Zuilen, M.A., and Bach, W., 2020, Mineral self-organization on a lifeless planet: *Physics of Life Reviews*, v. 34–35, p. 62–82, <https://doi.org/10.1016/j.plrev.2020.01.001>.
- Javaux, E.J., 2019, Challenges in evidencing the earliest traces of life: *Nature*, v. 572, p. 451–460, <https://doi.org/10.1038/s41586-019-1436-4>.
- Javaux, E.J., and Lepot, K., 2018, The Paleoproterozoic fossil record: Implications for the evolution of the biosphere during Earth's middle-age: *Earth-Science Reviews*, v. 176, p. 68–86, <https://doi.org/10.1016/j.earscirev.2017.10.001>.
- Kleinjan, W.E., de Keizer, A., and Janssen, A.J.H., 2005, Equilibrium of the reaction between dissolved sodium sulfide and biologically produced sulfur: *Colloids and Surfaces B: Biointerfaces*, v. 43, p. 228–237, <https://doi.org/10.1016/j.colsurfb.2005.05.004>.
- Lalonde, S.V., Konhauser, K.O., Reysenbach, A.L., and Ferris, F.G., 2005, The experimental silicification of Aquificales and their role in hot spring sinter formation: *Geobiology*, v. 3, p. 41–52, <https://doi.org/10.1111/j.1472-4669.2005.00042.x>.
- Larkin, J.M., and Strohl, W.R., 1983, *Beggiatoa*, *Thiothrix*, and *Thioploca*: *Annual Review of Microbiology*, v. 37, p. 341–367, <https://doi.org/10.1146/annurev.mi.37.100183.002013>.
- Lepot, K., Benzerara, K., Rividi, N., Cotte, M., Brown, G.E., Jr., and Philippot, P., 2009, Organic matter heterogeneities in 2.72 Ga stromatolites: Alteration versus preservation by sulfur incorporation: *Geochimica et Cosmochimica Acta*, v. 73, p. 6579–6599, <https://doi.org/10.1016/j.gca.2009.08.014>.
- Lepot, K., Addad, A., Knoll, A.H., Wang, J., Troadec, D., Béché, A., and Javaux, E.J., 2017, Iron minerals within specific microfossil morphospecies of the 1.88 Ga Gunflint Formation: *Nature Communications*, v. 8, 14890, <https://doi.org/10.1038/ncomms14890>.
- Lyons, T.W., Anbar, A.D., Severmann, S., Scott, C., and Gill, B.C., 2009, Tracking euxinia in the ancient ocean: A multiproxy perspective and Proterozoic case study: *Annual Review of Earth and Planetary Sciences*, v. 37, p. 507–534, <https://doi.org/10.1146/annurev.earth.36.031207.124233>.
- Marin-Carbonne, J., Remusat, L., Sforza, M.C., Thomazo, C., Cartigny, P., and Philippot, P., 2018, Sulfur isotope's signal of nanopyrates enclosed in 2.7 Ga stromatolitic organic remains reveal microbial sulfate reduction: *Geobiology*, v. 16, p. 121–138, <https://doi.org/10.1111/gbi.12275>.
- Marshall, C.P., Emry, J.R., and Olcott Marshall, A., 2011, Haematite pseudomicrofossils present in the 3.5-billion-year-old Apex Chert: *Nature Geoscience*, v. 4, p. 240–243, <https://doi.org/10.1038/ngeo1084>.
- McMahon, S., 2019, Earth's earliest and deepest purported fossils may be iron-mineralized chemical gardens: *Proceedings of the Royal Society [London]: B, Biological Sciences*, v. 286, 20192410, <https://doi.org/10.1098/rspb.2019.2410>.
- Raven, M.R., Sessions, A.L., Adkins, J.F., and Thunell, R.C., 2016, Rapid organic matter sulfurization in sinking particles from the Cariaco Basin water column: *Geochimica et Cosmochimica Acta*, v. 190, p. 175–190, <https://doi.org/10.1016/j.gca.2016.06.030>.
- Rickard, D., and Luther, G.W., 2007, Chemistry of iron sulfides: *Chemical Reviews*, v. 107, p. 514–562, <https://doi.org/10.1021/cr0503658>.
- Schopf, J.W., Kudryavtsev, A.B., Sugitani, K., and Walter, M.R., 2010, Precambrian microbe-like pseudofossils: A promising solution to the problem: *Precambrian Research*, v. 179, p. 191–205, <https://doi.org/10.1016/j.precamres.2010.03.003>.
- Schopf, J.W., Kudryavtsev, A.B., Walter, M.R., Van Kranendonk, M.J., Williford, K.H., Kozdon, R., Valley, J.W., Gallardo, V.A., Espinoza, C., and Flannery, D.T., 2015, Sulfur-cycling fossil bacteria from the 1.8-Ga Duck Creek Formation provide promising evidence of evolution's null hypothesis: *Proceedings of the National Academy of Sciences of the United States of America*, v. 112, p. 2087–2092, <https://doi.org/10.1073/pnas.1419241112>.
- Toporski, J.K.W., Steele, A., Westall, F., Thomas-Keptra, K.L., and McKay, D.S., 2002, The simulated silicification of bacteria—New clues to the modes and timing of bacterial preservation and implications for the search for extraterrestrial microfossils: *Astrobiology*, v. 2, p. 1–26, <https://doi.org/10.1089/153110702753621312>.
- Wacey, D., Kilburn, M.R., Saunders, M., Cliff, J., and Brasier, M.D., 2011, Microfossils of sulphur-metabolizing cells in 3.4-billion-year-old rocks of Western Australia: *Nature Geoscience*, v. 4, p. 698–702, <https://doi.org/10.1038/ngeo1238>.
- Wacey, D., McLoughlin, N., Kilburn, M.R., Saunders, M., Cliff, J.B., Kong, C., Barley, M.E., and Brasier, M.D., 2013, Nanoscale analysis of pyritized microfossils reveals differential heterotrophic consumption in the ~1.9-Ga Gunflint chert: *Proceedings of the National Academy of Sciences of the United States of America*, v. 110, p. 8020–8024, <https://doi.org/10.1073/pnas.1221965110>.
- Wacey, D., Noffke, N., Saunders, M., Guagliardo, P., and Pyle, D.M., 2018, Volcanogenic pseudo-fossils from the ~3.48 Ga Dresser Formation, Pilbara, Western Australia: *Astrobiology*, v. 18, p. 539–555, <https://doi.org/10.1089/ast.2017.1734>.

Printed in USA